Formal Hydride Transfer from NADH Analogues. 1-Benzyl-4-*tert*-butyl-1,4-dihydronicotinamide as a Mechanistic Probe

Agnès Anne,* Jacques Moiroux, and Jean-Michel Savéant

Contribution from the Laboratoire d'Electrochimie Moléculaire de l'Université de Paris 7, Unité Associée au CNRS No. 438, 2 place Jussieu, 75251 Paris Cedex 05, France

Received May 24, 1993[⊛]

Abstract: Direct and indirect (by means of ferrocene mediators) cyclic voltammetry and preparative-scale electrolyses of the title compound revealed that, even in the presence of bases, the resulting cation radical undergoes cleavage of the *t*-Bu· radical rather than proton abstraction. On the basis of this observation, the *tert*-butyl compound was used as a mechanistic probe, and it was shown that formal hydride transfer from *t*-BuBNAH to *p*-chloranil follows an electron-transfer reaction pathway. Implications for the hydride-transfer reactions of NADH analogues are discussed.

In spite of a large number of studies, there is still no general agreement on the mechanism of formal hydride transfer from models of the dihydronicotinamide coenzyme NAD(P)H to organic substrates, NAD^+ synthetic analogues,[17] flavins,[3] ketones,[2a,8-13] and quinones.[2a,11,13-21] The question of the distinctionbetween a direct one-step hydride transfer and a multistep electron–proton–electron, electron–hydrogen atom, or hydrogen atom–electron reaction is still open to debate, particularly for substrates containing carbonyl groups.

The ability of NADH analogues to act as one-electron donors, producing the cation radical as an intermediate, has been established through their reactions with one-electron oxidants,[2a,4,14,22-25] typically ferricyanide and ferrocenium ions, as well as by means of direct electron transfer with an anode.[26] On the basis of these reactions, the one-electron-oxidation formal potentials of NADH analogues have been determined in several cases.[4,14,22,25,26]

It has been argued in several instances that the observed rate constants are too large for an electron-transfer mechanism, the rate constant of which was estimated from thermodynamic data.[3,4,14,18,19,22,23] This approach may be illustrated by the oxidation of 1-benzyl-1,4-dihydronicotinamide ($BNAH_2$[27]) by *p*-chloranil (pCA) in acetonitrile, a reaction that will be particularly discussed in the following. The electron-transfer reaction

$$BNAH_2 + pCA \rightleftarrows BNAH_2^{\bullet+} + pCA^{\bullet-}$$

has a standard free energy of 0.770 eV (from $E^\circ_{BNAH_2^{\bullet+}/BNAH_2}$ = 0.780 V vs SCE[4,22,26c] and $E^\circ_{pCA/pCA^{\bullet-}}$ = 0.010 V vs SCE[5]). For such an uphill reaction, it may be assumed that the reverse electron-transfer rate constant is at the diffusion limit and, therefore, at 20 °C, that the forward rate constant should be 4.5 × 10^{-4} M^{-1} s^{-1}, i.e., 6.6 orders of magnitude smaller than the observed rate constant. However, one has to take into account that the interaction between $BNAH_2^{\bullet+}$ and the quinone anion radical may favor energetically the electron-transfer reaction. An attractive interaction of 0.40 eV (9 kcal/mol) would be required to justify the 6 orders of magnitude difference in rate

* Abstract published in *Advance ACS Abstracts*, September 15, 1993.

(1) (a) Roberts, R. M. G.; Ostovic, D.; Kreevoy, M. M. *Faraday Discuss. Chem. Soc.* **1982**, *74*, 257. (b) Kreevoy, M. M.; Kotchevar, A. T. *J. Am. Chem. Soc.* **1990**, *112*, 3579 and references cited therein.

(2) (a) Yasui, S.; Ohno, A. *Bioorg. Chem.* **1986**, *14*, 70 and references cited therein. (b) Ohno, A.; Shio, T.; Yamamoto, H.; Oka, S. *J. Am. Chem. Soc.* **1981**, *103*, 2045.

(3) Powell, M. F.; Bruice, T. C. *Prog. Clin. Biol. Res.* **1988**, *274*, 369.

(4) (a) Martens, F. M.; Verhoeven, J. W.; Gase, R. A.; Pandit, U. K.; de Boer, T. J. *Tetrahedron* **1978**, *34*, 443. (b) Verhoeven, J. W.; van Gerresheim, W.; Martens, F. M.; Van der Kerk, S. M. *Tetrahedron* **1986**, *42*, 975.

(5) Hajdu, J.; Sigman, D. S. *J. Am. Chem. Soc.* **1975**, *97*, 3524.

(6) Van Laar, A.; Van Ramesdonk, H. J.; Verhoeven, J. W. *Recl. Trav. Chim. Pays-Bas* **1983**, *102*, 157.

(7) Bunting, J. W. *Bioorg. Chem.* **1991**, *19*, 456.

(8) Shinkai, S.; Hamada, H.; Kusano, Y.; Manabe, O. *J. Chem. Soc., Perkin Trans. 2* **1979**, 699.

(9) Fukuzumi, S.; Mochizuki, S.; Tanaka, T. *J. Am. Chem. Soc.* **1989**, *111*, 1497.

(10) (a) Tanner, D. D.; Stein, A. R. *J. Org. Chem.* **1988**, *53*, 1642. (b) Tanner, D. D.; Kharrat, A. *J. Org. Chem.* **1988**, *53*, 1646. (c) Tanner, D. D.; Kharrat, A. *J. Am. Chem. Soc.* **1988**, *110*, 2968.

(11) (a) Martens, F. M.; Verhoeven, J. W.; Gase, R. A.; Pandit, U. K.; de Boer, T. J. *Tetrahedron* **1978**, *34*, 443. (b) Verhoeven, J. W.; van Gerresheim, W.; Martens, F. M.; van der Kerk, S. M. *Tetrahedron* **1986**, *42*, 975.

(12) (a) Steffens, J. J.; Chipman, D. M. *J. Am. Chem. Soc.* **1971**, *93*, 6694. (b) Chipman, D. M.; Yaniv, R.; Van Eikeren, P. *J. Am. Chem. Soc.* **1980**, *102*, 3244.

(13) Fukuzumi, S.; Ishikawa, M.; Tanaka, T. *Tetrahedron* **1986**, *42*, 1021.

(14) Carlson, B. W.; Miller, L. L. *J. Am. Chem. Soc.* **1985**, *107*, 479.

(15) (a) Fukuzumi, S.; Koumitsu, S.; Hironaka, K.; Tanaka, T. *J. Am. Chem. Soc.* **1987**, *109*, 305. (b) Fukuzumi, S.; Nishizawa, N.; Tanaka, T. *J. Org. Chem.* **1984**, *49*, 3571.

(16) Ohno, A.; Goto, M.; Mikata, Y.; Kashiwagi, T.; Maruyama, T. *Bull. Chem. Soc. Jpn.* **1991**, *64*, 87 and references cited therein.

(17) Tanner, D. D.; Kharrat, A.; Oumar-Mahamat, H. *Can. J. Chem.* **1990**, *68*, 1662.

(18) (a) Colter, A. K.; Saito, G.; Sharom, F. J. *Can. J. Chem.* **1977**, *55*, 2741. (b) Lai, C. C.; Colter, A. K. *J. Chem. Soc., Chem. Commun.* **1980**, 1115. (c) Colter, A. K.; Lai, C. C.; Williamson, T. W. *Can. J. Chem.* **1983**, *61*, 2544. (d) Colter, A. K.; Plank, P.; Bergsma, J. P.; Lahti, R.; Quesnel, A. A.; Parsons, A. G. *Can. J. Chem.* **1984**, *62*, 1780. (e) Colter, A. K.; Parsons, A. G.; Foohey, K. *Can. J. Chem.* **1985**, *63*, 2237.

(19) (a) Murray, C. J.; Webb, T. *J. Am. Chem. Soc.* **1991**, *113*, 7426. (b) - Coleman, C. A.; Rose, J. G.; Murray, C. J. *J. Am. Chem. Soc.* **1992**, *114*, 9755.

(20) (a) Fukuzumi, S.; Tanaka, T. *Chem. Lett.* **1982**, 1513. (b) Fukuzumi, S.; Nishizawa, N.; Tanaka, T. *Chem. Lett.* **1983**, 1755. (c) Fukuzumi, S.; Nishizawa, N.; Tanaka, T. *J. Org. Chem.* **1984**, *49*, 3571.

(21) (a) Fukuzumi, S.; Ishikawa, M.; Tanaka, T. *Chem. Lett.* **1989**, 1227. (b) Fukuzumi, S.; Ishikawa, M.; Tanaka, T. *J. Chem. Soc., Perkin Trans. 2* **1989**, 1811. (c) Ishikawa, M.; Fukuzumi, S. *J. Chem. Soc., Faraday Trans.* **1990**, *86*, 3531.

(22) Miller, L. L.; Valentine, J. R. *J. Am. Chem. Soc.* **1988**, *110*, 3892.

(23) Sinha, A.; Bruice, T. C. *J. Am. Chem. Soc.* **1984**, *106*, 7291.

(24) Brewster, M. E.; Simay, A.; Czako, K.; Winwood, D.; Farag, H.; Bodor, N. *J. Org. Chem.* **1989**, *54*, 3721.

(25) (a) Carlson, B. W.; Miller, L. L. *J. Am. Chem. Soc.* **1983**, *105*, 7453. (b) Carlson, B. W.; Miller, L. L.; Neta, P.; Grodkowski, J. *J. Am. Chem. Soc.* **1984**, *106*, 7233.

(26) (a) Hapiot, P.; Moiroux, J.; Savéant, J.-M. *J. Am. Chem. Soc.* **1990**, *112*, 1337. (b) Anne, A.; Hapiot, P.; Moiroux, J.; Neta, P.; Savéant, J.-M. *J. Phys. Chem.* **1991**, *95*, 2370. (c) Anne, A.; Hapiot, P.; Moiroux, J.; Neta, P.; Savéant, J.-M. *J. Am. Chem. Soc.* **1992**, *114*, 4694.

(27) Since the following study deals with 1-benzyl-4-*tert*-butyl-1,4-dihydronicotinamide, which will be designated by *t*-BuBNAH, leading upon formal hydride transfer to *t*-$BuBNA^+$, we have changed the traditional designation of 1-benzyl-1,4-dihydronicotinamide, BNAH, to $BNAH_2$.

0002-7863/93/1515-10224$04.00/0 © 1993 American Chemical Society

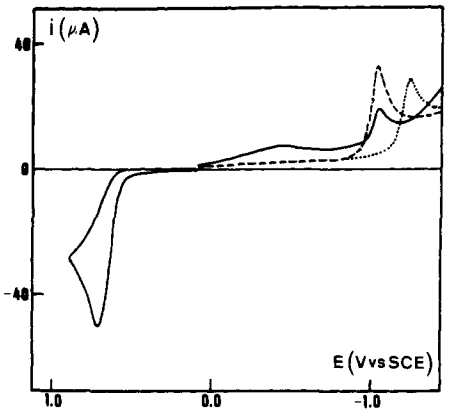

Figure 1. Solid line: cyclic voltammetry of *t*-BuBNAH (1.1 mM) in acetonitrile and 0.1 M *n*-Bu_4NBF_4 in the presence of 20 mM pyridine. The potential is scanned from 0.1 to 0.9 V and back to 0.1 V at 0.1 V/s and then from +0.1 to −1.45 V at 0.4 V. Dashed line: cyclic voltammetry of $BNAH^+$ (0.45 mM) in the same medium from +0.1 to −1.45 V at 0.4 V/s. Dotted line: cyclic voltammetry of *t*-$BuBNA^+$ (0.38 mM) in the same medium from +0.1 to −1.45 V at 0.4 V/s.

constants. This figure seems too large for a purely electrostatic interaction energy between the two ion radicals in the presence of other ions but might be reached if specific interactions were involved.

If interactions of this magnitude do exist between the ion radicals that result from electron transfer, the stereospecific reductions that have been observed would be consistent with an electron-transfer mechanism as well as a direct hydride-transfer mechanism.[2,16]

H–D kinetic isotope effects and isotope distribution in products do not always lead to clear-cut conclusions either. This is particularly the case with substrates containing a carbonyl group since, due to H–D scrambling in hydroxyl functions, isotope distribution is most often meaningless and the sole source of information resides in the kinetic isotope effects. With, for example, quinones, the observed kinetic H–D isotope effect has been interpreted either as the result of a direct hydride transfer[18,22] or as the result of a rate-determining proton transfer following an initial electron transfer step.[15]

As described in the following, we have found that the *t*-$BuBNAH^{\cdot+}$ cation radical produced upon oxidation by heterogeneous or homogeneous outer-sphere electron transfer undergoes, unlike $BNAH_2^{\cdot+}$,[26] cleavage of the 4-carbon–*tert*-butyl bond rather than deprotonation by bases present in the reaction medium. On the basis of this observation, we then used the *tert*-butyl compound as a mechanistic probe to test the occurrence of electron transfer in the reduction of quinones. We have taken *p*-chloranil as an example of the quinone compounds because the driving force for electron transfer is not too unfavorable, lending some credibility to the assumption that this pathway competes with the direct hydride-transfer pathway.

Results and Discussion

Direct and Indirect Electrochemical Oxidation of *t*-BuBNAH. The cyclic voltammetry of *t*-BuBNAH in acetonitrile (in the presence of *n*-Bu_4BF_4 as the supporting electrolyte) is summarized in Figure 1. It exhibits an oxidation wave which remains irreversible at all scan rates between 0.1 and 100 V/s. By comparison to the cyclic voltammetric oxidation of $BNAH_2$ under the same conditions (see ref 26 for a description of the electrochemical oxidation of $BNAH_2$), it is seen that the oxidation of *t*-BuBNAH consumes two electrons per molecule. The intermediacy of the cation radical *t*-$BuBNAH^{\cdot+}$ is indicated by the width of the cyclic voltammetric peak. It varies from 70 mV at 0.2 V/s to 90 mV at 20 V/s, showing[28] that the reaction is under the mixed rate control of the first electron transfer and a fast follow-up reaction. It would thus seem that the reaction is similar to the oxidation of $BNAH_2$, in which the first electron transfer is followed by the deprotonation of the cation radical.[26] That this is not actually the case is shown by the voltammogram obtained upon setting the initial potential of the scan beyond the oxidation peak and noting that the irreversible reduction wave observed upon cathodic scanning is not that of the reduction of *t*-$BuBNA^+$ but rather that of the reduction of $BNAH^+$, as can be seen by comparison with the voltammograms of authentic samples.

We have observed that the cyclic voltammograms thus obtained did not change significantly upon introduction of a buffer. The various buffers that have been tested in this respect are the same as those used in the investigation of the reaction of *t*-BuBNAH with *p*-chloranil, i.e., those listed in Tables I and II. We also noted that the introduction of bases rather than buffers did not produce any significant effect, showing that even under basic conditions, where $BNAH_2^{\cdot+}$ would be rapidly deprotonated, the formation of $BNAH^+$ still prevails over that of *t*-$BuBNA^+$.

The formation of $BNAH^+$ upon electrochemical oxidation of *t*-BuBNAH was confirmed by preparative-scale electrolysis. A 5 mM solution of *t*-BuBNAH in acetonitrile containing 10 mM collidine and 1 M H_2O was electrolyzed at a platinum electrode at 0.900 V vs SCE. Water was introduced into the solution to trap the *t*-Bu^+ carbocation possibly formed from *tert*-butyl alcohol. A temperature of 4 °C was used to increase the solubility of the volatile products possibly formed. Under these conditions, $BNAH^+$ was formed quantitatively after the consumption of 1.8 e/molecule as measured by cyclic voltammetry. *t*-BuOH (65–70%) and isobutene (7–8%) were detected by gas chromatography. The yield of the latter product is certainly underestimated, owing to its volatility.

It thus unambiguously appears that the cation radical produced upon direct electrochemical oxidation of *t*-BuBNAH

$$t\text{-BuBNAH} - e^- \rightleftarrows t\text{-BuBNAH}^{\cdot+} \qquad (1)$$

undergoes carbon–carbon cleavage in the 4-position rather than proton abstraction as $BNAH_2^{\cdot+}$ does. Among the two possible modes of cleavage, the formation of the *t*-Bu· radical and $BNAH^+$

$$t\text{-BuBNAH}^{\cdot+} \xrightarrow{k} t\text{-Bu}^{\cdot} + BNAH^+ \qquad (2)$$

has a driving force much larger than that of the converse formation of the *tert*-butyl carbocation and BNAH· (the driving force advantage is of the order of 1.2 eV[29]) and is thus likely to prevail.

However, as soon as it is formed, the *t*-Bu· radical is immediately oxidized to *t*-Bu^+, since its oxidation potential[29] is much less positive than the oxidation potential of *t*-BuBNAH. The formation of *t*-BuOH by reaction with water and of isobutene by deprotonation ensues. As will be seen next, the rate constant of reaction (2) is very large ($>10^8$ s^{-1}). It follows that the *t*-Bu· radical formed at the electrode surface has no time to react through dimerization and H atom disproportionation before being oxidized at the electrode by means of an "ECE" mechanism.[28b,30]

We also investigated the oxidation of *t*-BuBNAH by means of redox catalysis,[28b,31] i.e., by a homogeneous mediator, Q,

(28) (a) Nadjo, L.; Savéant, J.-M. *J. Electroanal. Chem. Interfacial Electrochem.* **1973**, *48*, 113. (b) Andrieux, C. P.; Savéant, J.-M. Electrochemical Reactions. In *Investigation of Rates and Mechanisms of Reactions*; Bernasconi, C. P., Ed.; Techniques of Chemistry; Vol. 6, Part 2; Wiley-Interscience: New York, 1986; pp 305–390.

(29) (a) The standard potential of the *t*-Bu^+/*t*-Bu· redox couple is 0.09 V vs SCE,[29b] and that of $BNAH_2^{\cdot}/BNAH_2^+$ is −1.105 mV vs SCE.[26c,29c] (b) Wayner, D. D. M.; McPhee, D. J.; Griller, D. *J. Am. Chem. Soc.* **1988**, *110*, 132. (c) Anne, A.; Hapiot, P.; Moiroux, J.; Savéant, J. M. *J. Electroanal. Chem. Interfacial Electrochem.* **1992**, *331*, 959.

(30) Amatore, C.; Gareil, M.; Savéant, J.-M. *J. Electroanal. Chem. Interfacial Electrochem.* **1984**, *176*, 377.

(31) Andrieux, C. P.; Hapiot, P.; Savéant, J.-M. *Chem. Rev.* **1990**, *90*, 723.

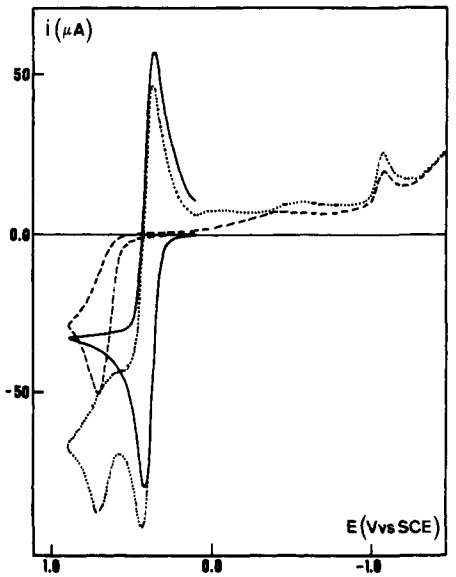

Figure 2. Redox catalysis of the oxidation of *t*-BuBNAH by ferrocenium ions in acetonitrile and 0.1 M *n*-Bu_4NBF_4 (temperature 20 °C): full line, ferrocene (2.3 mM) alone (scan rate 0.1 V/s); dashed line, *t*-BuBNAH (1.1 mM) (scan rate 0.1 V/s from 0.1 to 0.9 V, 0.4 V/s from +0.1 to −1.45 V); dotted line, mixture of the two (scan rate 0.1 V/s from 0.1 to 0.9 V, 0.4 V/s from +0.1 to −1.45 V).

generated at the electrode by oxidation of its reduced form, P (ferrocene, $E°_{PQ}$ = 0.405 V vs SCE, and (4-nitrophenyl)ferrocene, $E°_{PQ}$ = 0.523 V vs SCE, were used for this purpose).

$$P - e^- \rightleftarrows Q$$

$$Q + t\text{-BuBNAH} \underset{k_{-e}}{\overset{k_e}{\rightleftarrows}} P + t\text{-BuBNAH}^{\bullet+} \qquad (1')$$

$$t\text{-BuBNAH}^{\bullet+} \xrightarrow{k} t\text{-Bu}^{\bullet} + BNAH^+ \qquad (2)$$

$$Q + t\text{-Bu}^{\bullet} \rightarrow P + t\text{-Bu}^+ \qquad (3)$$

As shown in Figure 2, the introduction of *t*-BuBNAH into a solution of P renders the reversible P/Q cyclic voltammetric wave irreversible and increases its height as a result of reactions 1′–3. It is indeed seen (Figure 2) that the product of the oxidation of *t*-BuBNAH by the electrochemically generated ferrocenium ion is $BNAH^+$ and not *t*-$BuBNA^+$ as in the case of direct electrochemical oxidation. The same result was obtained in the presence of bases such as pyridine (pK_a = 12.3[32]) or *tert*-butylamine (pK_a = 18.2[32]), again showing that, even in the presence of rather strong bases, the carbon–carbon cleavage in the cation radicals still prevails over its deprotonation. From the variations of i_p/i_p^0 (peak currents of the mediator in the presence and absence of *t*-BuBNAH) with the scan rate (between 0.1 and 2 V/s) and the mediator concentration we inferred that the catalytic reaction is under the rate control of forward electron transfer (in reaction 1′). The corresponding rate constants k_e could then be derived by means of the appropriate theoretical working curves,[28,31,33] and the following values were found: log k_e = 2.34 ± 0.05 with ferrocene and log k_e = 4.22 ± 0.05 with (4-nitrophenyl)ferrocene. The variation of log k_e from one mediator to the other, 62 mV per unit, indicates that the reverse electron-transfer step (in reaction 1′) is under diffusion control, thus leading to a value for the standard potential of the *t*-$BuBNAH^{\bullet+}$/*t*-BuBNAH couple of 0.845 V vs SCE, slightly more positive than that of the $BNAH_2^{\bullet+}/BNAH_2$ couple, 0.786 V vs SCE.[26c] The very fact that the catalytic reaction is kinetically controlled by the forward electron-transfer step indicates that the cleavage reaction (reaction 2) is remarkably fast with a rate constant larger than 2×10^8 s^{-1}.[33]

Reduction of *p*-Chloranil by *t*-BuBNAH. Since rapid cleavage of the 4-C–C bond is the result of one-electron transfer from *t*-BuBNAH, we attempted to use this observation to detect the occurrence of electron transfer in formal hydride transfer from this reactant. *p*-Chloranil was selected as the substrate because the relatively high value of the pCA/pCA^- standard potential, 0.010 V vs SCE,[5] may allow electron transfer to compete with direct hydride transfer. Even in the absence of buffer and supporting electrolyte, we did not detect the presence of any charge-transfer complex between the two reactants at concentrations as large as 10 mM for *p*-chloranil and 40 mM for *t*-BuBNAH. In view of the slowness of the reaction, such a CT complex should have been, if present, easily detected. The kinetic and product distribution results we obtained with a first series of buffers, *polyhaloacetic acids and* CH_3SO_3H, are summarized in Table I. A mixture of three products was obtained, the relative amounts varying with the pH and the nature of the buffer components. Besides *t*-$BuBNA^+$ (**X**), which derives formally from the starting *t*-BuBNAH molecule by abstraction of $2e^-$ and $1H^+$ (or equivalently H^-), and $BNAH^+$ (**Y**) (abstraction of $2e^-$ + *t*-Bu^+), an addition compound, **Z**, whose structure is shown in Scheme I, was obtained (its identification is described in the Experimental Section). The analysis of the product distribution by means of cyclic voltammetry is illustrated in Figure 3; it was confirmed in some cases by HPLC. In all cases, the yield of **Z** was also determined by UV–vis spectrophotometry.

These results suggest the mechanism depicted in Scheme I. The fact that the half-reaction time is independent of the buffer acid whereas the product distribution strongly depends upon this factor indicates that product selection takes place after the rate determining step. The yields of **Y**, the product resulting from electron transfer and *t*-Bu· cleavage, decrease, as the yields of **X** and **Z** increase, from values close to 1 to 0, as the pH increases. At the highest edge of the pH range, the yields of **X** and **Z** are both 0.5. The latter observation suggests that, according to the mutual orientation of the cation and anion radicals resulting from the initial rate-determining electron-transfer step, either H atom transfer from the cation to the anion radical or carbon–carbon coupling leading to **Z** (after elimination of HCl) occurs. Under these conditions, the elimination of the *t*-Bu· radical from the cation radical, as observed in the direct and indirect electrochemical experiments, is disfavored by the interaction within the radical ion pair (see below) while H atom transfer is favored in one form of the radical ion pair and carbon–carbon coupling is favored in the other form of the radical ion pair. As the pH decreases, more and more of the cation radicals in the radical ion pairs protonate. The attractive interaction between the two radicals in the pair decreases accordingly, and elimination of the *t*-Bu· radical from the anion radical becomes sufficiently fast to outrun the formation of **X** and **Z** that are both disfavored by the lesser proximity of the two reacting molecules.

We may estimate, along the same lines as those in the introduction, what should be the product work term in the electron transfer between *p*-chloranil and *t*-BuBNAH corresponding to the observed value of the bimolecular rate constant, 0.1 M^{-1} s^{-1}. From the value of $E°_{t\text{-BuBNAH}^{\bullet+}/t\text{-BuBNAH}}$, 0.845 V vs SCE, and that of $E°_{pCA/pCA^{\bullet-}}$, 0.010 V vs SCE, the free energy of the electron-

(32) (a) Kolthoff, I. M.; Chantoni, M. K.; Bhownik, S. *J. Am. Chem. Soc.* **1968**, *90*, 23. (b) Coetzee, J. F. *Prog. Phys. Org. Chem.* **1967**, *4*, 76. (c) Cauquis, G.; Deronzier, A.; Serve, D.; Vieil, E. *J. Electroanal. Chem. Interfacial Electrochem.* **1975**, *60*, 205.

(33) (a) Andrieux, C. P.; Blocman, C.; Dumas-Bouchiat, J.-M.; Savéant, J.-M. *J. Am. Chem. Soc.* **1979**, *101*, 3431. (b) Andrieux, C. P.; Blocman, C.; Dumas-Bouchiat, J.-M.; M'Halla, F.; Savéant, J.-M. *J. Electroanal. Chem. Interfacial Electrochem.* **1980**, *113*, 19. (c) Andrieux, C. P.; Blocman C.; Dumas-Bouchiat, J.-M.; M'Halla, F.; Savéant, J.-M. *J. Am. Chem. Soc.* **1980**, *102*, 3806. (d) Andrieux, C. P.; Savéant, J.-M. *J. Electroanal. Chem. Interfacial Electrochem.* **1986**, *205*, 43. (e) Andrieux, C. P.; Anne, A.; Moiroux, J.; Savéant, J.-M. *J. Electroanal. Chem. Interfacial Electrochem.* **1991**, *307*, 17.

Table I. Reaction of *t*-BuBNAH with *p*-Chloranil in Polyhaloacetic and Methanesulfonic Acid Buffers[a]

buffer acid	pK_a log K_h[b]	pH[d]	compn [A]/[B][f]	$t_{1/2}$[g] (min)	product yields[h] X	Y	Z	$k_0 \approx k'_0$ (M^{-1} s^{-1})	k_1/k_2[k] (M)	k_3/k'_2[k]
CH_3SO_3H	10.0[c] 3.8[c]	10.0[e]	20.0/20.0	35	0.38	0.62	0.00	0.1	0.004	0.01
CF_3CO_2H	12.9	10.7	78.7/20.5	35	0.07	0.93	0.00[i]			
	3.0	13.4	9.8/13.1	35	0.35	0.15	0.50	0.1	0.005	13.6
		14.0	9.9/20.1	35	0.40	0.10	0.50			
		14.9	9.7/39.9	35	0.45	0.05	0.50			
CHF_2CO_2H	16.2	12.5	20.0/0.5	35	0.43	0.56	0.02			
	3.8	13.2	20.0/2.0	35	0.43	0.32	0.25[j]			
		13.8	19.3/5.3	35	0.42	0.30	0.28	0.1	0.097	345
		14.6	19.3/13.3	35	0.46	0.08	0.46			
		16.2	10.0/10.0	35	0.48	0.02	0.50[j]			
$CHCl_2CO_2H$	16.2	14.3	17.1/7.8	35	0.40	0.20	0.40	0.1	0.1	320
	3.8	16.2	20.0/20.0	35	0.48	0.02	0.50			

[a] Initial concentrations are [*t*-BuBNAH] = 2 mM and [*p*-chloranil] = 1 mM, unless otherwise stated, in acetonitrile and 0.1 M *n*-Bu_4NBF_4 at 20 °C. [b] K_h is the homoconjugation equilibrium constant in M^{-1}; pK_a and log K_h were determined in the present work (see Experimental Section) unless otherwise stated. [c] From ref 32b. [d] ±0.3 unless otherwise stated. [e] ±0.1. [f] Concentrations of acid and base (in mM) introduced into the solution. [g] Half-reaction time. [h] Assayed by means of cyclic voltammetry unless otherwise stated; the yield of **Z** was assayed spectrophotochemically in all cases. [i] [*t*-BuBNAH] = 4 mM; [*p*-chloranil] = 2 mM. [j] Assayed by means of HPLC and cyclic voltammetry. [k] Average values; see text and Figure 4.

transfer reaction, 0.835 eV, should lead to a rate constant of 4 × 10^{-5} instead of 0.1 M^{-1} s^{-1}. The free energy of interaction in the radical ion pair may thus be estimated as 0.2 eV (4.7 kcal/mol), a quite reasonable value, taking into account that it includes an electrostatic and a π/π^* attractive component.

There is good agreement between the experimental distribution of products and the predictions of the mechanism depicted in Scheme I, as can be seen in Figure 4. The predicted variations of the **X** and **Z** yields were simulated by taking the homoconjugation equilibrium into account. The values of the rate constant ratios, k_1/k_2 and k_3/k'_2, for each acid ensue (Table I).

Nearly the same values of k_1/k_2 are obtained for CH_3SO_3H and CF_3CO_2H whereas k_1/k_2 increases upon passing to CHF_2CO_2H and $CHCl_2CO_2H$ (which have the same pK_a). These observations indicate that, with the first two acids, the rate of protonation of the quinone is close to the diffusion limit. As expected, it then slowly decreases upon passing to acids of higher pK_a.

With *pyridine and substituted pyridines*, the products **X** and **Y** are again obtained, the formation of **Y** being also favored at the expense of **X** as the pH decreases (Table II). The most significant difference from reactions with the previous series of acids is the absence of **Z** among the reaction products in all cases but that of the sterically encumbered 2,6-di-*tert*-butyl-4-methylpyridine. The reason for the disappearance of **Z** is not known with certainty but may be related to the formation, when steric hindrance is not too severe, of a π/π^* complex between the cation radical of the radical ion pair and the pyridine molecule. In the resulting complex, the reversible carbon–carbon coupling would be less than in the absence of the pyridine whereas, in the other form of the radical ion pair, H atom transfer would be favored by the ensuing interaction between *t*-$BuBNA^+$ and the pyridine. Protonation of the quinone anion radical still triggers the elimination of *t*-Bu· from the cation radical, but stronger acidic media than those used with the previous series of buffers are required to outrun H atom transfer. As the pH increases, as with pyridine, 3-methylpyridine, and 3,5-dimethylpyridine, the relative amounts of **X** and **Y** tend toward a steady value, 57:43, indicating that, in the I branch of the reaction scheme (Scheme I), H atom transfer has totally overcome the *t*-Bu· cleavage reaction. In this series, the J branch of the reaction scheme remains irreversible, as indicated by the observation that the half-reaction time remains the same. The values of the rate constants of the two parallel electron transfer steps leading to I and J are only slightly different, 0.12 and 0.10 s^{-1}, respectively. As the most basic pyridine of the series is reached, the formation of **X** further increases at the expense of **Y**. This observation may be interpreted as follows.

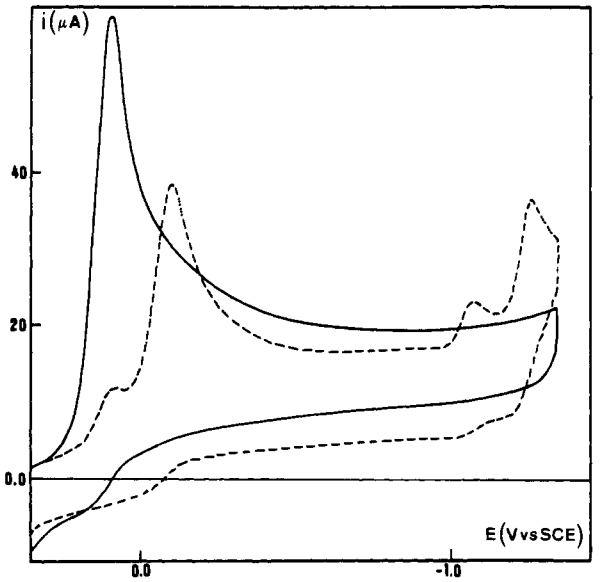

Figure 3. Reaction of *p*-chloranil (1 mM) with *t*-BuBNAH (2mM) in acetonitrile and 0.1 M *n*-Bu_4NBF_4. Determination of the product distribution by means of cyclic voltammetry (temperature 20 °C, scan rate 0.2 V/s): full line, *p*-chloranil alone; dashed line, the mixture after 130 min.

The increase in pH renders the formation of **Y** in the J branch less and less efficient to the point that it ceases to compete with the reverse electron-transfer step (as noted earlier, the electron-transfer reaction is an uphill process). Then, the J branch of the reaction scheme progressively shuts down as branch I becomes more predominant. This interpretation is confirmed by the fact that the half-reaction time increases, tending, as expected, toward a value twice that observed at lower pH.

Conclusions

The main conclusion to emerge from the above results and discussion is that, using the cleavage of *t*-Bu· in the oxidation of *t*-BuBNAH by *p*-chloranil as a mechanistic probe, electron transfer may be, as previously hypothesized,[2,15,20] the first step of the formal hydride-transfer reaction of NADH analogues. The reaction we investigated has, however, the particularity that the two reactants are such that electron transfer, although uphill, is not too disfavored from a thermodynamic point of view. When the driving force for electron transfer is less, direct hydride transfer may well be the preferred reaction pathway. This might be the case even with *p*-chloroanil as the hydride acceptor and seems to

Scheme I

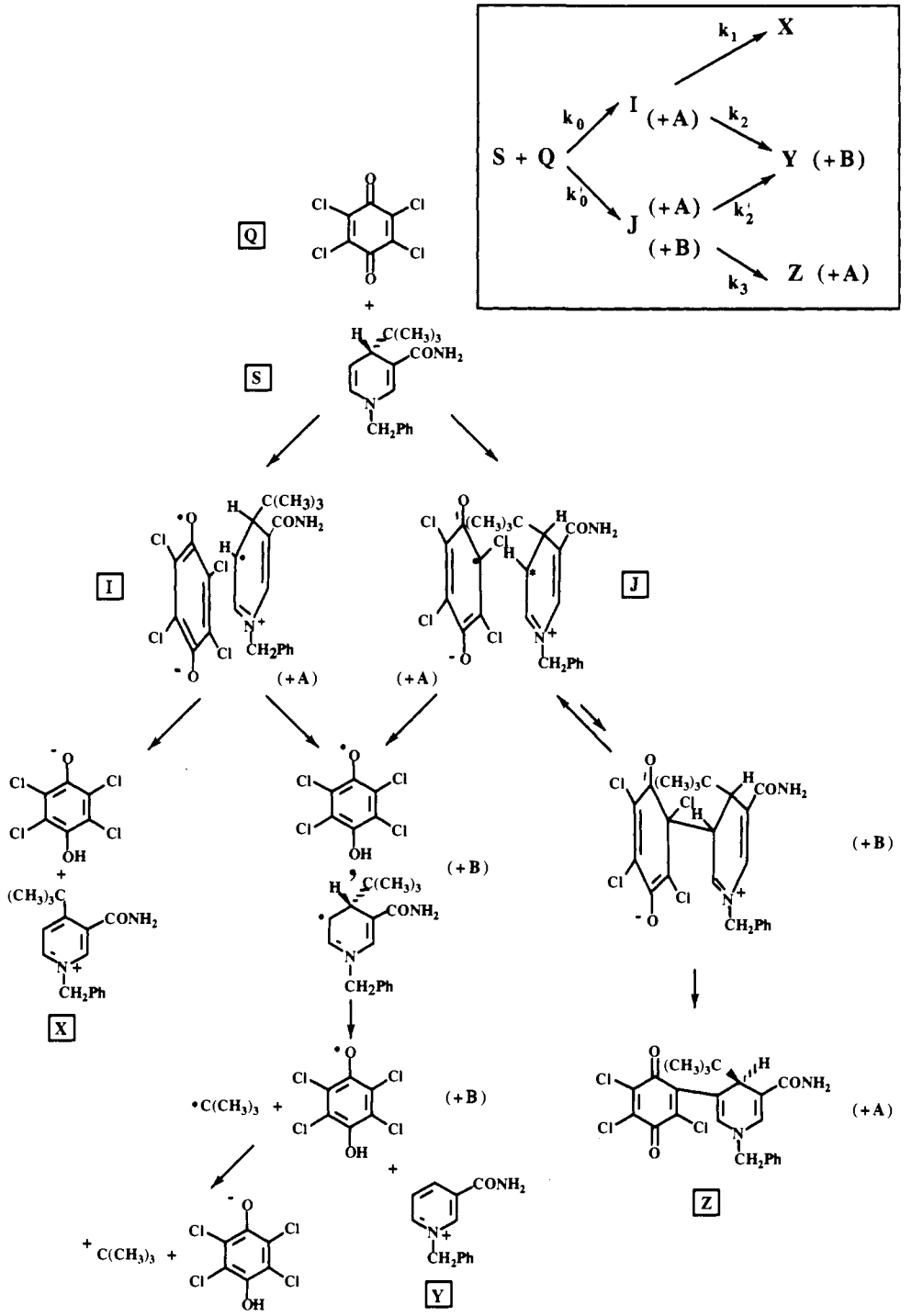

be actually the case when *p*-chloranil is opposed to $BNAH_2$, a system in which the electron-transfer mechanism has been deemed to operate. By comparison with the values estimated here, the interaction free energy in the successor complex required to match the experimental value of the rate constant is indeed too large (0.4 instead of 0.2 e V) for an electron-transfer mechanism. The large value of the H–D kinetic isotope effect found for this reaction[15] points to the same conclusion. As shown in the present study, the H atom transfer reaction following the initial electron transfer step is sufficiently fast to render the latter step rate-determining. With $BNAH_2$, the reaction is less uphill than in the present case and therefore the initial electron transfer should be rate-determining as well. It follows that the observed kinetic isotope effect is not compatible with the electron-transfer mechanism.

Thus, although observed in particularly favorable circumstances, it may well be that the electron-transfer mechanism plays a marginal role in formal hydride-transfer reactions of NADH analogues.

Another point worth noting is the importance of low-energy molecular interactions in product selection, as illustrated by the differences in product distribution resulting from changes in the natures of the buffers and bases.

Experimental Section

Chemicals. 1-Benzyl-4-*tert*-butyl-1,4-dihydronicotinamide (*t*-BuBNAH),[34] 1-benzylnicotinamidinium chloride,[35] 1-benzyl-1,4-dihydroni-

(34) Anne, A. *Heterocycles* **1992**, *34*, 2331.
(35) Mauzerall, D.; Westheimer, F. M. *J. Am. Chem. Soc.* **1955**, *77*, 2261.

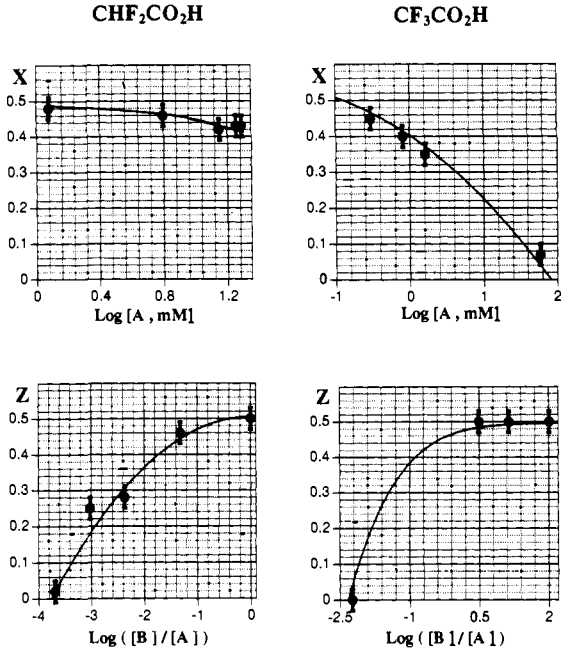

Figure 4. Experimental (dots) and predicted (lines) distributions of products (Y = 1 − X − Z) according to Scheme I with the rate parameters listed in Table I.

Table II. Reaction of *t*-BuBNAH with *p*-Chloranil in Pyridine Buffers[a]

buffer base	pH[b]	compn [A]/[B][d]	$t_{1/2}$[e] (min)	product yields[f] X	Y	Z
3-F-pyridine	9.4[c]	20.0/20.0	28	0.05	0.95	0.00
4-$CONH_2$-pyridine	10.1[c]	20.0/20.0	30	0.33	0.67	0.00
pyridine	12.2[c]	30.0/20.0	30	0.42	0.58	0.00[g]
	12.6[c]	10.0/20.0	30	0.33	0.67	0.00[g]
3-Me-pyridine	13.3[c]	30.0/20.0	32	0.57	0.43	0.00[g]
	13.5[c]	20.0/20.0	32	0.57	0.43	0.00[g]
	13.8[c]	10.0/20.0	32	0.57	0.43	0.00[g]
3,5-Me_2-pyridine	15.0	10.0/20.0	33	0.57	0.43	0.00
2,4,6-Me_3-pyridine	15.0	20.0/5.0	36	0.70	0.30	0.00
	15.6	20.0/20.0	36	0.70	0.30	0.00
	16.3	5.0/19.9	48	0.90	0.10	0.00
2,6-*t*-Bu_2-4-Me-pyridine	12.8	20.0/20.0	30	0.43	0.56	0.12
	13.8	20.0/50.6	30	0.43	0.56	0.12[g]

[a] Initial concentrations are [*t*-BuBNAH] = 2 mM and [*p*-chloranil] = 1 mM, in acetonitrile and 0.1 M *n*-Bu_4NBF_4 at 20 °C. [b] ±0.2; $pK_{a,AH}$ determined in the present work (see Experimental Section) unless otherwise stated. [c] ±0.1; pK_{a,AH^+} from ref 32. [d] Concentrations of acid and base (in mM) introduced into the solution. [e] Half-reaction time. [f] Assayed by means of cyclic voltammetry unless otherwise stated; the yield of **Z** was assayed by spectrophotometry in all cases. [g] Assayed by means of HPLC and cyclic voltammetry.

cotinamide,[35] and (*p*-nitrophenyl)ferrocene[26c,36] were prepared as previously reported. *n*-Bu_4BF_4 was from Fluka. Acetonitrile (Spectrosol purity grade, 50 mM H_2O) and deuteriated solvents were obtained from SDS. Other chemicals were Aldrich Chemical Co. commercial products of the highest available purity. All chemicals were used as received. Fresh solutions were prepared before each experiment.

Instruments. Spectroscopic and electrochemical instruments were the same as previously described.[26,29c,34]

Chromatography. Gas chromatography was performed on a Delsi 30MCV gas chromatograph equipped with an ionization detector, utilizing a 5% OV17 on ChromosorbW 100/200 stainless steel column (2.1-mm i.d. × 5 m) and a Shimadzu C-R6A integrating recorder. Isobutene and *tert*-butyl alcohol, formed during electrochemical oxidation of *t*-BuBNAH solutions, were analyzed by GC at 60 °C (retention times were 4.3 min for isobutene and 6.4 min for *tert*-butyl alcohol, eluted before the acetonitrile peak). The yields of these compounds were determined by comparing the integrated GC peak areas to those of the authentic samples with reference to calibration curves. In the case of isobutene, calibration was established after bromine titration of the pure sample in CCl_4.[37]

High-performance liquid chromatography was performed with a Gilson gradient system equipped with a Gilson variable-wavelength UV–visible detector and a Spectra Physics SP4290 integrator. A reverse-phase Hypersil C_{18} ODS2 stainless steel column (4.6 mm i.d. × 25 cm, 5 μm particle size) preceded by a Hypersil C_{18} guard column was used for the analyses. The mobile phases were CH_3CN/H_2O (20/80 v/v) (A) and CH_3CN/H_2O (80/20 v/v) (B) containing 0.02 M NH_4OAc. The gradient consisted of a 5-min linear step from 15% to 5% B, followed by a 15-min linear step to 100% B, a 5-min isocratic step with 100% B, and a 5-min linear step to initial conditions (15% B). The flow rate was 1.0 mL min^{-1}. The course of the reaction of *t*-BuBNAH with *p*-chloranil was monitored by periodically removing 0.5-mL aliquots and diluting them with 0.5 mL of the HPLC eluent A, containing phenol as an internal standard for experiments carried out in polyhaloacetic buffers. When precipitation of the unreacted quinone occurred, samples were filtered through a cotton plug before HPLC analysis. Peaks were identified at 265 nm by comparison of elution times with those of authentic samples. Quantitations of the final products, $BNAH^+$ (HPLC retention time (t_r) = 16.1 min), *t*-$BuBNA^+$ (t_r = 18.1 min), **Z** (t_r = 22.5 min), and unreacted *t*-BuBNAH (t_r = 19.1 min), were determined by means of their integrated peak areas relative to those of phenol (t_r = 8.3 min) or with respect to calibration curves of integrated peak area versus concentration.

For preparative-scale HPLC separations, a Waters μ-Bondapak C_{18} stainless steel column (7.8-mm i.d. × 25 cm, 10-μm particle size) was employed. Compounds were eluted isocratically at a flow rate of 2.0 mL min^{-1}, the mobile phase being composed of $H_2O/CH_3CN/CH_3OH$ mixtures.

Buffer Preparations. The pyridine buffers were prepared by introducing adequate amounts of base and $HClO_4$ (11.67 M aqueous solution) into the background solution. Polyhaloacetic and methanesulfonic acid buffers were prepared similarly by mixing the acid and tetramethylammonium hydroxide pentahydrate.

Determinations of pK_a's. The pK_a's of the polyhaloacetic acids A_i with A_1 = CF_3COOH, A_2 = CHF_2COOH, and A_3 = $CHCl_2COOH$ were determined by reaction with pyridine derivatives. For A_1, the base was pyridine, and for both A_2 and A_3, the base was 2,4,6-trimethylpyridine. The concentrations of protonated (PyH^+) and unprotonated pyridine (Py) derivatives at equilibrium were measured spectrophotometrically. The initial concentrations of A_i and Py introduced into 0.1 M *n*-Bu_4BF_4 acetonitrile were $C^0_{A_i} = C^0_{Py} = C^0 = 2$ mM. Under these conditions, the fraction x of PyH^+ was always >0.5. Since A_i and its deprotonated form B_i are known to associate and produce A_iB_i with a homoconjugation equilibrium constant $K_{h,i} = (A_iB_i)/(A_i)(B_i)$, which is usually large,[32a,b] the reaction between A_i and Py can be written as

$$A_i + Py \rightarrow B_i + A_iB_i + PyH^+$$

and the concentration (A_i), compared with (B_i) and (A_iB_i), is very small at equilibrium. Hence $(PyH^+) = C^0x$, $(Py) = C^0(1-x) = (A_iB_i)$, $(B_i) = C^0(2x-1)$, and $K_{a,i}/K_{h,i} = (H^+)C^0(2x-1)^2/(1-x)$ with $(H^+) = (K_{a,PyH^+})x/(1-x)$ since the association between Py and PyH^+ is negligible.[32a,b] Respective values of 15.9, 19.9, and 20.2 were found for $\log(K_{a,i}/K_{h,i})$, where i = 1–3. For uncharged acids, the difference between the pK_a values in acetonitrile and dimethyl sulfoxide is 9.7–10 and the homoconjugation equilibrium constant is small in DMSO.[32a] The pK_a of A_3 is 6.4 in the latter solvent.[38] That gives $pK_{a,3} = 16.2 \pm 0.3$ and $\log K_{h,3} = 3.8$ in acetonitrile. Taking into account all causes of uncertainty, it seems reasonable to consider that $pK_{a,2} = pK_{a,3}$ and $\log K_{h,2} = \log K_{h,3}$, since $\log(K_{a,3}/K_{h,3})$ and $\log(K_{a,2}/K_{h,2})$ do not differ by more than 0.3 unit. As $pK_{a,CH_3COOH} = 22.3$ and $\log K_{h,CH_3COOH} = 4.7$,[32a,b] it appears that $K_{h,i}$ decreases with decreasing $pK_{a,i}$ and we can approximate $pK_{a,1}$ and $\log K_{h,1}$ as 12.9 ± 0.3 and 3.0, respectively.

The pK_a of protonated 2,6-di-*tert*-butyl-4-methylpyridine (PyH^+) depends markedly on the solvent and the background composition.[39] In

(36) Beckwith, A. L. J.; Leydon, R. J. *Aust. J. Chem.* **1966**, *19*, 139.

(37) (a) Siggis, S. *Quantitative Organic Analysis of Functional Groups*; Wiley: New York, 1954; p 68. (b) Fritz, J. S; Hammond, G. S. *Quantitative Organic Analysis*; Wiley: New York, 1957; p 275.

(38) Bordwell, F. G. *Acc. Chem. Res.* **1988**, *21*, 456.

(39) (a) Brown, H. C.; Kanner, B. *J. Am. Chem. Soc.* **1966**, *88*, 986. (b) Aue, D. H.; Webb, H. M.; Bowers, M. T.; Liotta, C. L.; Alexander, C. J.; Hopkins, H. P. *J. Am. Chem. Soc.* **1976**, *98*, 854. (c) Hopkins, H. P.; Ali, S. Z. *J. Am. Chem. Soc.* **1977**, *99*, 2069. (d) Arnett, E. M.; Chawla, B. *J. Am. Chem. Soc.* **1978**, *100*, 214. (e) Hopkins, H. P.; Jahagvidar, D. V.; Moulik, P. S.; Aue, D. H.; Webb, H. M.; Davidson, W. R.; Pedley, M. D. *J. Am. Chem. Soc.* **1984**, *106*, 4341.

order to determine such a pK_a in the media used in the present study, we took advantage of the fact that Py reacts with the protonated form of *p*-toluidine (TH^+) to yield PyH^+ and T, the concentrations (Py), (PyH^+), (T), and (TH^+) being comparable at equilibrium. With a mixture of equal concentrations ($C^0 = 5$ mM) of Py, T, and $HClO_4$ in the background solution, the equilibrium concentration C^0x of T was determined spectrophotometrically. The associations between bases and acids of the B and BH^+ type are known to be relatively weak[32a,b] and were neglected. Then pK_{a,PyH^+} was deduced from the experimental determination of the ratio $K_{a,TH^+}/K_{a,PyH^+} = x^2/(1-x)^2$ since $pK_{a,TH^+} = 11.25$ is given in the literature.[32b] We found $pK_{a,PyH^+} = 12.8 \pm 0.2$. For collidine (2,4,6-trimethylpyridine), we proceeded similarly. Collidine, morpholine ($pK_a = 16.6$),[32b] and $HClO_4$ were mixed at the same initial concentrations of 2.5 mM. The concentrations of collidine and its protonated form at equilibrium were determined spectrophotometrically. We found $pK_a = 15.6 \pm 0.2$, a value lower than that of 16.8 given in ref 32c.

Reaction of *t*-BuBNAH with *p*-Chloranil. The reaction of *t*-BuBNAH with quinones in buffered acetonitrile was investigated under selected experimental conditions so as to ensure that none of the reactants or final products taken separately undergoes any noticeable decomposition over a period corresponding to at least five half-reaction times, as was checked with authentic samples. It was found that under deaerated conditions, the pH range extending from 9.0 to 16.5 was compatible with stabilities both of the dihydronicotinamide reactant *t*-BuBNAH and of the quinones and pyridinium products, which are respectively acid- and base-unstable compounds. The concentrations of the buffer components were chosen to be suitably efficient to maintain the pH at a nearly constant value during the reactions (see Tables I and II); their concentrations were usually varied up to the solubility limit, or to the limit at which the overlap of the signals due to the buffer components and those of the compounds of interest becomes significant. At pH values lower than 12, UV–visible spectrophotometry evidenced that *t*-BuBNAH ($\lambda_{max} = 320$ nm, $\epsilon_{max} = 5400\ M^{-1}\ cm^{-1}$) could be protonated in acetonitrile with a pK_a of 8.6 ± 0.2 to give a species ($\lambda_{max} = 356$ nm, $\epsilon_{max} = 10800\ M^{-1}\ cm^{-1}$) highly sensitive to the presence of air. Electrochemical and spectrophotometric studies showed that the protonated form of *t*-BuBNAH underwent a clean transformation in aerated media to afford the dealkylated pyridinium $BNAH^+$ as the final product. Typically, *p*-chloranil (1 mM) was dissolved in a thoroughly deaerated solution of buffered 0.1 M n-Bu_4BF_4/acetonitrile. Then *t*-BuBNAH (2 mM) was added to the solution, and the mixture was allowed to react at 20 °C in the dark under a stream of nitrogen. The progress of the reaction was followed by cyclic voltammetry and/or by HPLC (as described earlier). The conversion of the quinone was deduced from the decrease of its two-electron cathodic peak; the formation of the quinone adduct **Z** was derived from the measurement of the height of its two-electron cathodic peak compared with that of the initial quinone. The yield of the adduct **Z** was also confirmed by monitoring the increase of its visible absorption band at 674 nm. The formations of the pyridinium compounds $BNAH^+$ and *t*-$BuBNA^+$ were identified by comparison with those of authentic samples and were quantified from the increases in their respective one-electron cathodic peaks. When experiments were carried out in pyridinium-type buffers, measurements were performed after careful neutralization of the medium with tetraethylammonium acetate.

1-Benzyl-4-*tert*-butyl-5-(3,5,6-trichloro-2-*p*-benzoquinonyl)-1,4-dihydronicotinamide (Z). In a typical experiment, *p*-chloranil (17.7 mg, 9 mM) was allowed to react at room temperature under nitrogen, with two equivalent amounts of *t*-BuBNAH (29 mg, 13.5 mM) in CH_3CN or CD_3CN (8 mL) containing difluoroacetic acid/tetramethylammonium difluoroacetate (18 mM/18 mM). The initial yellow color turned intense blue with time. After completion of the reaction (*ca.* 1 h), acetonitrile was partially removed with a stream of nitrogen; then the crude reaction mixture was filtered through a cotton plug to remove a white precipitate of crude dihydro-*p*-chloranil. For the experiment using CD_3CN, the resulting filtrate was shown by ^1H NMR spectroscopy to contain the two pyridinium products $BNAH^+$ and *t*-$BuBNA^+$ in a *ca.* 30/70 ratio and the unreacted *t*-BuBNAH and the dihydronicotinamide adduct **Z** in equimolar amounts, proof that the products contained in the reaction mixture are the same as those identified after separation and purification. Such ratios were respectively based on measurements of the signals due to the H-4 proton and to the *C-4-tert*-butyl protons. Subsequent HPLC separation on the Waters column using the mobile phase $H_2O/CH_3CN/CH_3OH$ (100/300/50) gave a deep blue fraction (12–14 min) which was collected at this point. This fraction was then subjected to further purification using the same mobile phase, affording **Z** as a blue powder: ^1H NMR (230 MHz; CD_3CN) δ 7.40–7.36 (m, 6H, C_6H_5 and H-6), 7.25 (s, 1H, H-2), 5.84 (bs, 2H, NH_2), 4.62 (s, 2H, NCH_2), 3.83 (s, 1H, H-4), 0.63 (s, 9H, $C(CH_3)_3$); UV–vis (CH_3CN) λ_{max} (nm) (ϵ_{max} ($M^{-1}\ cm^{-1}$)) 658 (2100), 336 (5200), 274 (10400); CI–MS (NH_3) *m/z* (relative abundance) 485 (5, $[^{37}Cl_3]MH^+$), 483 (38, $[^{37}Cl_2,^{35}Cl]MH^+$), 481 (100, $[^{37}Cl,^{35}Cl_2]MH^+$), 479 (92, $[^{35}Cl_3]MH^+$), 427 (52, $[^{37}Cl_3]M - t$-Bu), 425 (10, $[^{37}Cl_2,^{35}Cl]M - t$-Bu), 423 (21, $[^{37}Cl,^{35}Cl_2]M - t$-Bu), 421 (15, $[^{35}Cl_3]M - t$-Bu). The detailed isotopic abundance pattern for the parent ion included peaks at 486 (1, $MH^+ + 7$), 484 (9, $MH^+ + 5$), 482 (38, $MH^+ + 3$), and 480 (26, $MH^+ + 1$) and was in excellent agreement with that expected for the molecular formula $C_{23}H_{21}O_3N_2Cl_3$ ($E^\circ_{Z^{\cdot}/Z}(CH_3CN) = -170 \pm 5$ mV vs SCE).